Time-Dependent Mechanical Behavior of a Granular Medium Used in Laboratory Investigations

Hani Ghiabi[1] and A. P. S. Selvadurai[2]

Abstract: The time-dependent mechanical response of an artificial granular medium consisting of glass beads is experimentally examined by performing one-dimensional creep tests on both saturated and dry specimens. The time-dependent compression of the oedometric sample, which is related to the internal rearrangement of the granular assembly, is modeled using an elastic-viscoplastic strain hardening constitutive model. The procedures used to identify the parameters defining the model are discussed; the incremental strain of the material is decomposed into reversible elastic and irreversible creep components. Finally, the capabilities of the proposed model in predicting the time-dependent response of the material are investigated through a comparison between experimental results and analogous results derived from computational modeling.

DOI: 10.1061/(ASCE)1532-3641(2009)9:1(1)

CE Database subject headings: Constitutive models; Creep; Granular media; Compression tests; Viscoplasticity; Laboratory tests.

Introduction

The mechanical behavior of granular materials is generally assumed to be time independent, although in many cases continued settlement of structures constructed on granular regions has been reported in the literature (Nonveiller 1963; Komornik et al. 1972; Sweeney and Lambson 1991; Hannink 1994). Time-dependent behavior in granular media can be attributed to several processes including progressive particle breakage due to intergranular contact stresses and the rearrangement of the grains with time due to micromechanical slip. The former processes that occur either under high overburden stresses or high confining stresses result in more angular particles, and on occasion lead to the development of more rounded grains mixed with fine grained materials (Yamamuro and Lade 1993; Leung et al. 1996; Lade and Liu 1998, Cheng et al. 2001). The latter processes that occur at shorter time scales of the order of days are important, particularly when granular materials at low relative densities are used in laboratory investigations (Murayama et al. 1984; Lade 1994; Di Prisco and Imposimato 1996; Kuwano and Jardine 2002). Oda (1972) conducted a series of drained triaxial tests on sand that mainly consisted of quartz grains. Photo-microphotographs from thin sections of sheared specimens revealed that the shearing process causes a continuous reconstitution of the initial fabric, by the sliding of grains along unstable contacts and the rolling of grains relative to a preferred reorientation. Murayama (1983) proposed a mechanical model to simulate the time-dependent stress–strain behavior of soil media, including coarse grained soil and caused by deviatoric stress. This model was then used to predict the creep behavior of sand specimens by appeal to the results obtained from experiments (Murayama et al. 1984). Conducting triaxial compression tests on the samples prepared from Toyoura sand, it was shown that the volumetric changes in the specimens ceased almost within 20 min.

In practical situations, creep phenomena lead to a gradual increase in the shear strength of the field deposits or the increase of the resistance with time (Mitchell and Solymar 1984; Schmertmann 1991). This hypothesis was investigated by Lade (1994), who conducted an experimental research program on Sacramento River sand. Allowing the triaxial samples to creep under drained conditions for various time periods, it was shown that the granular material achieved a stiffer state the longer the creep phenomenon was allowed to take place.

Another experimental study, involving a series of drained standard triaxial compression tests was conducted by Di Prisco and Imposimato (1996) on loose Hostun sand ($D_r \approx 20\%$). The results clearly showed that the material strain response to an instantaneous stress increment exhibits a delay with time; this time-dependent behavior was not due to stress transfer from the pore water to the soil skeleton, but to a change in the microstructural configuration of the sand resulting from the rotation and sliding of grains along the unstable contacts. Lade and Liu (1998) also presented the results of a series of isotropic compression and triaxial compression tests, concluding that the viscous characteristics of the granular media results from slippage between grains as well as fracture of the particles, especially under high confining pressures. Similar observations are reported by Gajo et al. (2000), who also provide additional references.

Kuwano and Jardine (2002) observed significant creep deformations in a series of triaxial tests under isotropic and anisotropic stress conditions conducted on sand and ballotini glass beads with $D_{50}=0.27$ mm. Their results showed that creep in a granular material is related to the gradual stabilization of the medium through

[1]Graduate Student, Dept. of Civil Engineering and Applied Mechanics, McGill Univ., Room 492, Macdonald Engineering Bldg., 817 Sherbrooke St. West, Montreal PQ, Canada H3A 2K6. E-mail: hani.ghiabi@mail.mcgill.ca

[2]William Scott Professor and James McGill Professor, Dept. of Civil Engineering and Applied Mechanics, McGill Univ., Rm. 492, Macdonald Engineering Bldg., 817 Sherbrooke St. West, Montreal PQ, Canada H3A 2K6. E-mail: patrick.selvadurai@mcgill.ca

Note. Discussion open until July 1, 2009. Separate discussions must be submitted for individual papers. The manuscript for this paper was submitted for review and possible publication on December 21, 2006; approved on March 17, 2008. This paper is part of the ***International Journal of Geomechanics***, Vol. 9, No. 1, February 1, 2009. ©ASCE, ISSN 1532-3641/2009/1-1–8/$25.00.

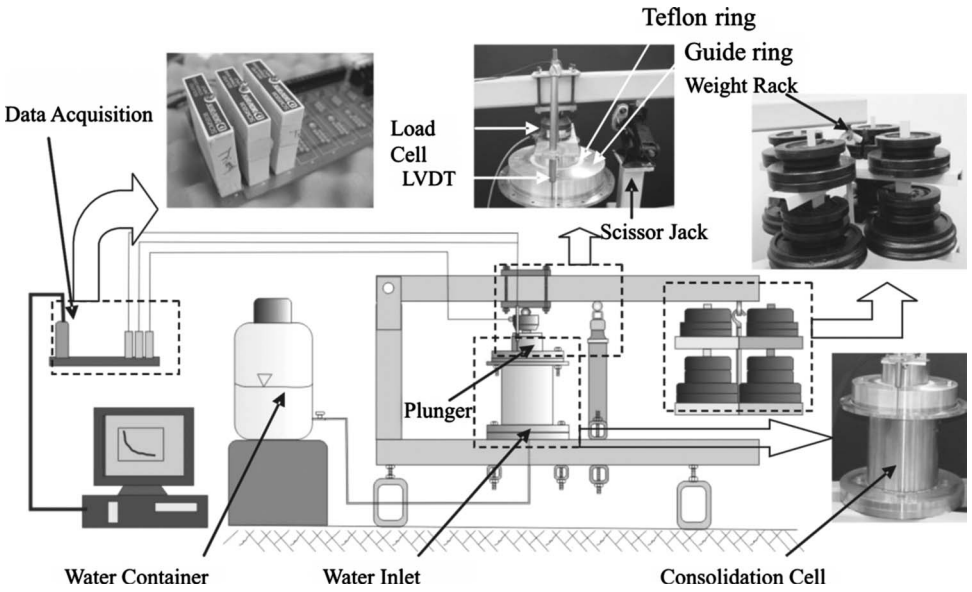

Fig. 1. Loading setup used in the bench-scale test

failure of the most critically loaded regions and, as a result, load transfer between the constituent grains.

Di Benedetto et al. (2002) studied the viscous properties of two types of clean sand (Hostun sand with D_{50}=0.31 mm and Toyoura sand with D_{50}=0.18 mm), conducting drained plane strain compression tests on rectangular-prismatic specimens. Their experimental studies showed significant viscous effects in either creep and stress relaxation stages, or during a change in the strain rate. Nawir et al. (2003) used an automated triaxial apparatus to examine the viscous response of cuboidal prismatic specimens of Toyoura sand under triaxial compression conditions. The identical viscous responses obtained from saturated and dried specimens reconfirmed that the time-dependent response of the specimens was primarily due to the fabric rearrangement of the grains, with negligible effects from the delayed dissipation of excess pore pressure. Recently, AnhDan et al. (2006) experimentally evaluated the viscous behavior of the gravelly soils following the methods used by Di Benedetto et al. (2002) and Nawir et al. (2003) for sandy samples. They observed similar time-dependent properties in partially saturated and fully saturated specimens, indicating that the time-dependent responses can be regarded as an intrinsic property of the soil skeleton, resulting from micromechanical phenomena at the fabric level.

In the present study, the time-dependent response of artificial glass beads (i.e., ballotini) was investigated by conducting bench-scale one-dimensional creep tests. The time-dependent behavior of the ballotini is examined using the viscoplastic model proposed by Perzyna (1966) along with the special assumptions that permit the definition of the hardening parameters and the flow function made by Lemaître and Chaboche (1996). The constitutive parameters applicable to the model are estimated using the experimental data derived from the one-dimensional creep tests. The time-dependent creep effects in ballotini are examined through computational modeling of the one-dimensional compression tests.

Experimental Investigations

Ballotini, an artificial particulate medium consisting of glass beads, is used in a wide range of industrial applications, including the cleaning, shot-peening, and finishing process for metal surfaces. Ballotini type A3 with a specific gravity estimated at 2.5, manufactured by Potters Industries Inc. (La Prairie, Que., Canada) was used for this experimental study. Grain size analysis indicated that 83% of this granular material ranged from 600 to 850 μm, whereas 17% had a particle size ranging between 300 and 600 μm.

In order to investigate the time-dependent response of the ballotini, two oedometric compression tests were carried out on a bench-scale apparatus containing the ballotini sample (Fig. 1). In the first experiment, the granular sample was saturated prior to loading, whereas in the second test the ballotini sample was maintained in a dry condition. A comparison of the results obtained from these tests highlights the influence of fabric rearrangement, under both dry and saturated conditions, on the time-dependent compression of the ballotini.

In these experiments, the axial stress was imposed by a dead load applied to the end of a lever arm. To eliminate the friction between the plunger and internal surface of the consolidation cell, an aluminum ring was attached to the cell to guide the plunger through the cell and to prevent the contact between the surfaces (Fig. 1). Further, to facilitate the vertical movement of the plunger, a Teflon ring was mounted on the inner part of the guide ring to minimize the friction in the system. The internal surface of the stainless steel cylinder also has a smooth finish to minimize the side friction during the axial compression of the specimen. The tests were performed on specimens with the dimensions of 168 mm in height and 152 mm in diameter. The initial dry density of the material was estimated at 1.54 g/cm^3 with a void ratio of 0.62. The specimens were fabricated by placing the ballotini in the oedometric cell in four layers; each layer was poured after noncompaction leveling of the surface of the previously placed layer.

In the test conducted on the saturated sample, adequate drainage was ensured by placing geotextile layers (F-300, Texel Inc.) at the upper and lower surfaces of the sample. After the fabrication of the specimen and prior to the application of the load, water was allowed to flow into the cell through the bottom inlet connected to a water reservoir. An initial hydraulic gradient close to unity was used in the saturation stage and the water level was

Int. J. Geomech., 2009, 9(1): 1-8

maintained at the upper surface of the specimen for 24 h. The specimens were subjected to a priming stress of magnitude 81 kPa, resulting from the test arrangement used to apply the axial load (i.e., the weight of the plunger, the lever arm, and the weight rack). Conducting a study on the influence of stress level on physical properties of nonwoven polyester geotextiles, Palmeira and Gardoni (2002) indicated that geotextile layers can be compressed to approximately 0.35 of the initial thickness under the normal pressure of 1,000 kPa. Further, a significant part of the compression of the geotextile (80–90% of this compression) takes place at normal stresses up to 100 kPa. Thus it is assumed that a significant portion of the compression of the geotextile layers, with initial thickness of 1.2 mm, took place during the application of the priming stress, whereas the geotextile compression that occurs during the application of the five main loading increments was considered to be negligible. This fact was also verified by comparing the compression response of the saturated sample with that of dry specimen, in which no geotextile was placed at the top and bottom of the sample. Upon application of the initial stress, the void ratio of the specimen decreased from an initial value of 0.62 to approximately 0.61. During the experiment, the axial stress was increased, successively, to 149, 219, 273, 383, and 493 kPa and was maintained constant at each level for a period of approximately 1 day.

The instrumentation used in the experimental setup included a load cell located on the top of the plunger and two LVDTs arranged to measure the vertical compression of the sample. The load cell used in this experiment has a capacity of 10 kips (44.48 kN) with an accuracy equal to $\pm 0.04\%$ FS. Further, the accuracy of the signal conditioning block is $\pm 0.08\%$ span. Considering the sensitivity of the load cell (4.11 mV/V), the resolution of the system is estimated at 0.027 kN, which is higher than the accuracy of the load cell. This resolution corresponds to approximately 1.5 kPa, which is regarded as an acceptable accuracy for this series of experiments. Two LVDTs, with a displacement range of 2.5 cm, were attached to diametrically opposite sides of the plunger to record the average vertical compression of the specimen. The 10 V excitation voltage required for the transducers was supplied from the rack of the signal conditioner module (ISO-RACK8), which can be connected to eight signal conditioning blocks. In these tests, three signal conditioner blocks with a gain of 50 converted the transmitted signals to high-level analog voltage outputs after a filtering and amplification process. These output voltages were then transferred to a desktop computer through a USB-based DAQ module (PMD-1606FS). Due to the higher rate of axial displacement during the initial stages of the load increments, readings were taken every second during the first hour of each load step. The data acquisition rate was then reduced to one reading per minute during the remainder of the load step, where a lower rate of axial compression was observed.

The time-dependent variation of the void ratio at different stress levels is indicative of the viscous-type processes within the oedometer sample. Fig. 2 clearly indicates that the reduction in void ratio of the saturated ballotini sample subjected to an instantaneous stress increment has a delayed response. It is important to note that full drainage was ensured by connecting the lower and upper surfaces of the specimen to the water inlet and draining vent, respectively. Considering the high hydraulic conductivity of the granular ballotini ($\approx 1.6 \times 10^{-3}$ cm/s), this particular time-dependent behavior is completely unrelated to any processes resulting from transient pore water pressure dissipation effects. Consequently, this phenomenon can only be attributed to the mechanical response of the skeleton that results from the rearrangement of the fabric at the contact locations. This fact was verified by conducting similar tests on dry samples of ballotini, where an identical behavior in the axial strain response was observed.

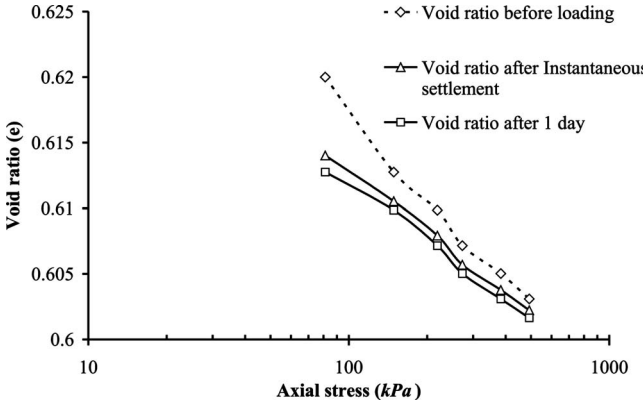

Fig. 2. Time variation of the void ratio in the oedometer test (saturated sample)

A part of the results of the tests conducted on a saturated sample was used to develop a generalized three-dimensional elastic-viscoplastic model capable of predicting the time-dependent mechanical response of the material. The proposed model was then used to predict the time-dependent effects in the remaining experiments.

Modeling of Time-Dependent Phenomena

Constitutive modeling of the time-dependent behavior observed in the experiments with ballotini uses the theory of viscoplasticity formulated by Perzyna (1966). The constitutive response of the material is developed by considering the decomposition of the strain rate into its reversible elastic and irreversible strain rates. As the oedometric compressive strains are not large, the additive decomposition (see, e.g., Desai and Siriwardane 1984; Davis and Selvadurai 1996) can be written as

$$\dot{\varepsilon}_{ij} = \dot{\varepsilon}^e_{ij} + \dot{\varepsilon}^c_{ij} \tag{1}$$

where $\dot{\varepsilon}^e_{ij}$ and $\dot{\varepsilon}^c_{ij}$=tensors of the *elastic strain rate* and the *viscoplastic strain rate*, respectively. The elastic strain rate can be defined through Hooke's law as follows:

$$\dot{\varepsilon}^e_{ij} = C^e_{ijmn}\dot{\sigma}'_{mn} \tag{2}$$

where C^e_{ijmn}=elastic compliance tensor and σ'_{mn}=tensor of effective stress. As pore fluid pressures encountered in the experimental configuration are assumed to have no influence on the mechanical response of the granular fabric, $\sigma'_{ij}=\sigma_{ij}$. The irreversible strain rate that combines both the irreversible and viscous responses is given by the following relationship:

$$\dot{\varepsilon}^c_{ij} = A\langle\Phi(F)\rangle\frac{\partial G}{\partial \sigma_{ij}} \tag{3}$$

where A=viscosity coefficient of the material, G=viscoplastic potential; F=static yield function; and Φ=flow function. The function F represents the overstress concept containing a plastic function and a strain hardening parameter. Assuming isotropic hardening of the material, the static yield function is represented in the form

Int. J. Geomech., 2009, 9(1): 1-8

$$F(\sigma_{ij},\varepsilon^c_{mn}) = \frac{f(\sigma_{ij},\varepsilon^c_{mn})}{\kappa(\tilde{\varepsilon}^c)} - 1 \tag{4}$$

where $f(\sigma_{ij},\varepsilon^c_{mn})$=plastic function; $\kappa(\tilde{\varepsilon}^c)$=hardening parameter; and $\tilde{\varepsilon}^c$=*equivalent irreversible (creep) strain* defined as

$$\dot{\tilde{\varepsilon}}^c = \left(\tfrac{2}{3}\dot{\varepsilon}^c_{ij}\dot{\varepsilon}^c_{ij}\right)^{1/2} \tag{5}$$

Assumptions can be implemented to further simplify the constitutive expressions (3) and (4); by considering an associated flow rule, the viscoplastic potential G will correspond to the yield function f. If one further assumes a von Mises type criterion to define the yield condition in the ballotini material, the plastic potential can be represented in terms of the equivalent deviatoric stress q in the following form:

$$G(\sigma_{ij}) = q = \sqrt{3J_{2D}} = \sqrt{\tfrac{3}{2}S_{ij}S_{ij}} \tag{6}$$

where J_{2D}=second invariant of the deviatoric stress tensor S_{ij}. Other yield criteria and hardening rules can be invoked to construct a more elaborate constitutive model; the objective here is to propose a canonical representation in terms of the von Mises criterion and to establish how accurately such a model can withstand a parameter identification and calibration exercise only for modeling time-dependent behavior observed in oedometric compression tests. Several laws can be postulated for the flow law Φ (see, e.g., Cristescu and Suliciu 1982; Desai and Zhang 1987; Selvadurai and Sepehr 1999). In this study, the flow function and the hardening parameter proposed by Lemaître and Chaboche (1996), is adopted, which take the forms

$$\Phi(F) = \left(\frac{F+1}{q^*}\right)^n \tag{7}$$

$$\kappa(\tilde{\varepsilon}^c) = (\tilde{\varepsilon}^c)^{-m/n} \tag{8}$$

where q^*=reference stress used to achieve a normalized equation for the rate of plastic strain. Thus, the irreversible viscoplastic strain rate, which accounts for both irreversible and viscous effects, is given by

$$\dot{\varepsilon}^c_{ij} = \tfrac{3}{2}Aq^{n-1}(q^*)^{-n}(\tilde{\varepsilon}^c)^m S_{ij} \tag{9}$$

and the equivalent rate of plastic strain $\dot{\tilde{\varepsilon}}^c$ is given by

$$\dot{\tilde{\varepsilon}}^c = \sqrt{\frac{2}{3}\dot{\varepsilon}^e_{ij}\dot{\varepsilon}^c_{ij}} = A\left(\frac{q}{q^*}\right)^n (\tilde{\varepsilon}^c)^m \tag{10}$$

where n=stress exponent and m=strain hardening parameter.

In order to describe the constitutive behavior of the ballotini, the parameters of the above-mentioned viscoplastic model were determined through the following parameter identification exercise: these constitutive parameters were determined from the results of the oedometer tests. Eq. (9) indicates that for uniaxial loading, the viscoplastic strain increment in the radial direction $d\varepsilon^c_{rr}$ is half of the strain increment in the axial direction $d\varepsilon^c_{zz}$, i.e.

$$d\varepsilon^c_{rr} = -\tfrac{1}{2}d\varepsilon^c_{zz} \tag{11}$$

Considering this relationship between the viscoplastic strain increments, the equivalent rate of viscoplastic strain can be obtained using the following relationship:

$$\dot{\tilde{\varepsilon}}^c = \sqrt{\frac{2}{3}\dot{\varepsilon}^c_{ij}\dot{\varepsilon}^c_{ij}} = \dot{\varepsilon}^c_{zz} \tag{12}$$

The equivalent viscoplastic strain in the creep test can be evaluated from Eq. (9) considering $\dot{\tilde{\varepsilon}}^c$ estimated from Eq. (12).

In the following section, the procedure used to obtain the material constants from the results of the compression test on a saturated specimen is discussed. Finally, the parameters derived using this exercise are used to predict the time-dependent uniaxial compression of the ballotini subjected to higher axial stress.

Identification of the Parameters for Lemaître's Model

The total strain in each load step was assumed to consist of a reversible elastic strain and an irreversible viscoplastic strain. To obtain the parameters of the elastic-viscoplastic model, the viscoplastic part has to be separated from the total deformation of the sample. The progressive deformation of the material can be investigated by subjecting the ballotini samples to two loading–unloading cycles; one conducted in a short time duration (instantaneously) and the other performed in longer time period. In the bench-scale test, the immediate loading–unloading of the specimens is not feasible due to the experimental technique used to apply the static constant stress, using dead weights. Therefore, isotropic compression tests were performed in the triaxial setup in which the volumetric compression and expansion of the saturated specimens can be obtained from the volume of the pore fluid extruded from or entered into the samples. In each load increment, two different phases were observed in the volume compression of the samples; the first phase corresponded to immediate volume reduction followed by a time-dependent compression process. In this test, two loading-unloading cycles were conducted on the triaxial specimens prepared with different initial void ratios; in the first cycle, the chamber pressure was increased to 500 and 600 kPa without allowing for time-dependent compression. The loading and unloading processes in this cycle were conducted in approximately 30 s in which the immediate volume change of the specimens was recorded at different confining pressures (Fig. 3). In the second cycle, the chamber pressure was maintained after each increase in chamber pressure (pressure increments of 100 kPa) for a period of approximately 5 min in both loading and unloading parts. It was observed that after the immediate deformation, the specimens exhibited further time-dependent compression. Further, results indicated that during the first cycle, the sample showed small irreversible volumetric strain after the complete unloading, whereas in the second cycle, higher magnitudes of irreversible compression were observed in the samples. Thus, it can be noted that a significant portion of the deformation that occurred during the instantaneous loading–unloading cycle can be considered as reversible elastic deformation. In other words, the irreversible compression of the samples can be regarded as a time-dependent process that takes place after the instantaneous elastic response of the samples.

In calculation of the elastic modulus, considering the fact that the irreversible strains develop after the initial elastic compression, the elastic radial strain at the time of the stress increase is assumed to be zero. At each load step, the elastic modulus of the sample was obtained from the instantaneous axial deformation that occurs after the load increment. After the third load step, the immediate axial deformation of the sample indicates that Young's modulus increases with the increase in the stresses, with a consequent decrease in the void ratio. This variation of the elastic modulus was also observed in the consolidated-drained (CD) triaxial tests conducted on ballotini specimens, compacted to various void ratios e_i under different confining pressures σ_C. From the results of the CD triaxial tests performed on ballotini, the Pois-

Int. J. Geomech., 2009, 9(1): 1-8

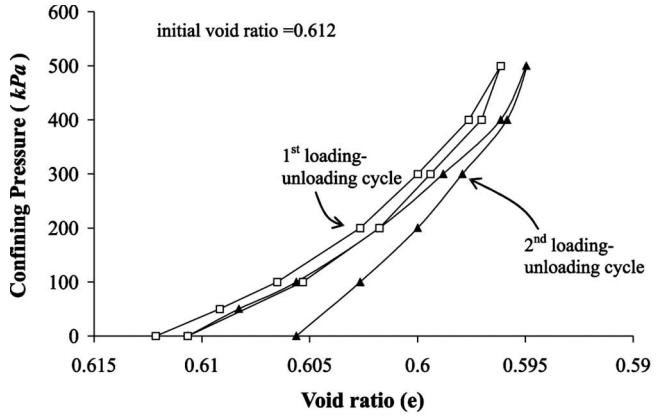

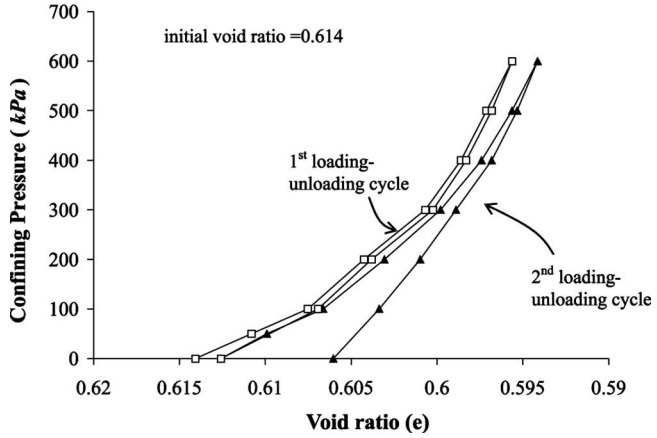

Fig. 3. Results of the isotropic compression test on two samples of ballotini

son's ratio (ν) of the material was also estimated at 0.3. Thus, the magnitude of the viscoplastic strain is estimated using

$$d\varepsilon_{zz}^{c} = d\varepsilon_{zz} - \left(\frac{d\sigma_{zz}}{E} - \frac{2\nu d\sigma_{rr}}{E}\right) \tag{13}$$

During the straining process, the viscoplastic strain in the radial direction increases; therefore, the radial stress gradually increases to maintain the total radial strain equal to zero. This evolution of the radial stress decreases the magnitude of axial elastic strain (ε_{zz}^{e}) with time. Therefore, in each load step, the parameters are determined by assuming a value for the radial stress. These parameters were then used in the numerical model of the problem to obtain the new stresses applied to the specimen. The ultimate parameters were obtained after several iterations of the computational procedure.

Considering the rate of irreversible strain at each load, the equivalent viscoplastic strain used to derive the parameters was evaluated from the plastic strains taking place in the same load

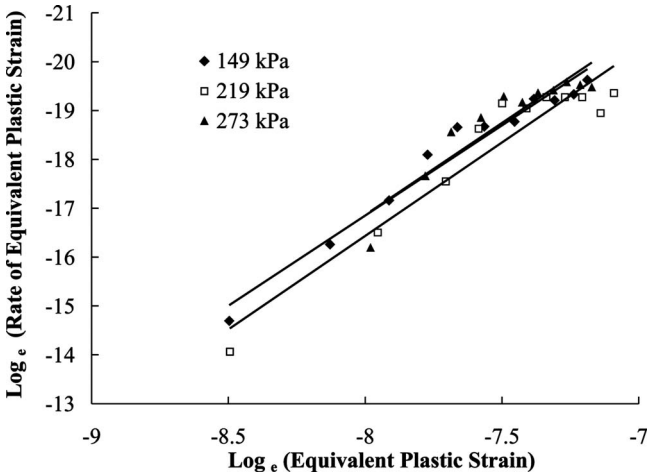

Fig. 4. Results of the uniaxial compression test at different load steps

step. In order to determine the strain hardening parameter (m), the rate of equivalent viscoplastic strain is plotted against the equivalent plastic strain in a logarithmic plot (Fig. 4). The slope of the curves represents the strain hardening parameter, which can be evaluated for different load steps.

In this diagram (Fig. 4), the intercept on the $\log_e$ (rate of equivalent viscoplastic strain) axis gives the viscosity parameter A, which depends on the stress exponent n and reference stress q^*. Considering a constant value for the stress exponent ($n=5$) and the deviator stress at failure for confining pressure equal to 300 kPa as the reference stress ($q^*=979$ kPa), the magnitude of the viscosity parameter can be estimated from the results of each load step. A summary of the elastic-viscoplastic parameters derived from the first three load steps using this procedure is presented in Table 1.

Implementation of the Elastic-Viscoplastic Model in the Computational Analysis

In order to validate the procedure used to estimate the constitutive parameters, the oedometric compression test was examined by using the nonlinear finite-element code (ABAQUS) and by modeling the cylindrical specimen as an axisymmetric region (S is the axis of symmetry) (Fig. 5). The steel plunger that constrained the upper boundary of the specimen to a uniform settlement was also modeled by considering a stiffer part compared to the granular sample ($E=10^7$MPa, $\nu=0.3$). For this analysis, the model of the specimen was discretized into 560 eight-node biquadratic axisymmetric quadrilateral elements, which were formulated on the basis of a reduced integration scheme. Each node in this element has two degrees of freedom corresponding to the displacement in the radial and vertical directions. The region was subjected to axial stresses equal to those applied in the experiments to the confined

Table 1. Summary of the Parameters Estimated from Three Load Steps (Saturated Sample)

Number of the load step	Modulus of elasticity (MPa)	Axial stress (kPa)	Strain hardening parameter, m	Stress exponent, n	Viscosity coefficient, A (s^{-1})
1	36.2	149	−3.85	5	1.18E−15
2	36.2	219	−3.84	5	8.33E−16
3	36.2	273	−3.80	5	3.19E−16

Int. J. Geomech., 2009, 9(1): 1-8

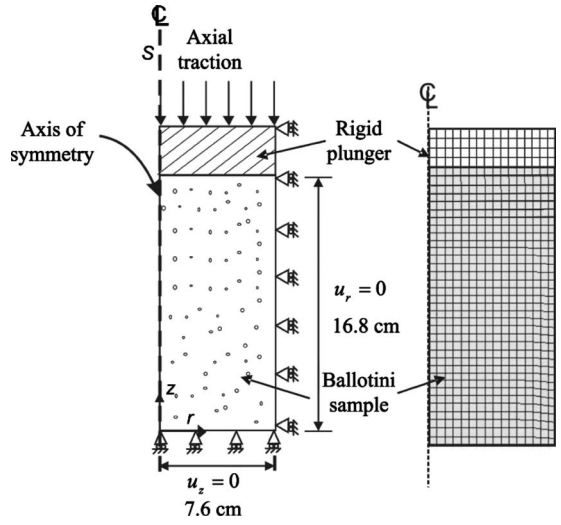

Fig. 5. Finite-element mesh and the model of the cylindrical sample implemented in the computational analysis

sample. Each load was maintained for a period of 1 day and the stress condition at the end of this period was considered as the initial condition for the next load step.

The comparison between the experimental and computational modeling for the three load steps is shown in Fig. 6. In each graph, the variation in the axial strain at different load steps is compared with the numerical result. The comparison indicates that, although the model parameters were derived from the experimental results conducted on saturated ballotini, the model reasonably predicts the time-dependent response of both saturated and dry specimens.

Validation of the Elastic-Viscoplastic Model

The parameters of the proposed viscoplastic model were determined from the experimental results obtained from the first three load steps. The capability of this model to simulate the oedometric compression process can be evaluated by predicting the material behavior under different stress conditions. For this reason, the elastic-viscoplastic model was implemented in the computational modeling of the oedometric compression test. Using results from the first three load steps, the parameters of the viscoplastic model were defined as $m=-3.81$, $q^*=979$ kPa, $n=5$, and $A=7.72\times10^{-16}$ s^{-1}. Conducting a sensitivity analysis on the range of parameters shown in Table 1, the selected values give rise to better numerical results for the first three load steps. The estimation of the elastic modulus of the material based on the presented method showed a nearly constant value in the first three load steps with an increase calculated in higher stress levels. Thus, the elastic modulus of the material is defined as a function of maximum principal stress σ_1; 36.2 MPa for σ_1 less than 273 kPa, and 45.7 and 56.0 MPa at σ_1 equal to 383 and 492.6 kPa, respectively. The next step in the validation of the model is the prediction of the time-dependent compression of the material in the last two load steps, which were not utilized for the estimation of the parameters. A comparison of the experimental results with the computational simulations is shown in Fig. 6; although there is a slight discrepancy between the results, it can be observed that the trends associated with the viscous compression of the granular sample can be well predicted. It is shown that the evolution of the void ratio during the compression process shows the same linear relationship between creep strain with log time at constant axial stress as that observed in other experimental studies (see, e.g., Leung et al. 1996; Lade and Liu 1998). Furthermore, the comparison indicates that the time-dependent axial strain of ballotini, which is less than 0.2% in each load step, can be reasonably simulated by the Lemaître viscoplastic model.

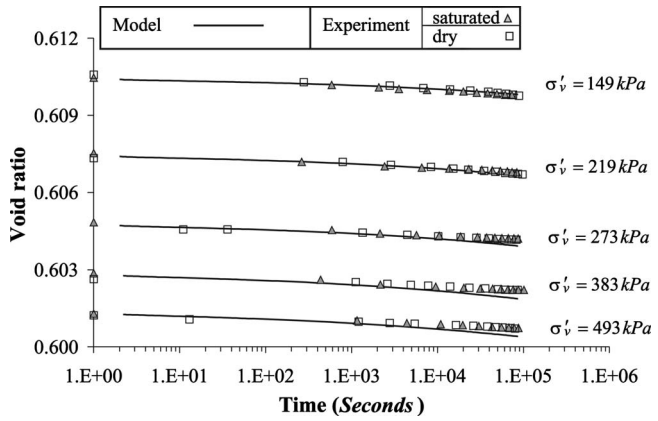

Fig. 6. Time-dependent oedometric compression of the ballotini in five load steps

Conclusions

The present study evaluated the time-dependent compression of ballotini, where the viscous behavior of the material was investigated by means of oedometer tests conducted on saturated and dry granular specimens. The existence of viscosity effects in the material was confirmed at different loading steps by recording the axial compression of the granular sample in a period of approximately 1 day. Effects of this nature are important in accurately interpreting results of either laboratory-scale model tests or other elemental tests, where additional deformations can result from the type of creep phenomena discussed in the paper, within the time frame of an experiment. The situation related to the long term (100 or 1,000 year) creep behavior is an important phenomenon and in these circumstances, the creep at grain contacts themselves will be important, and cannot be addressed through the viscoplastic model presented here. The phenomenon that is being described is viscoplasticity of the fabric rather than that of the individual grains at contact locations, which can lead to processes such as fusion of the grain contacts, depending on the stress states encountered.

The crushing process of the constituent grains, discussed in the Introduction, becomes important for angular particles that are more susceptible to breakage than rounded particles. For ballotini composed of rounded grains, the stress levels considered in this study are less than those needed to reach particle crushing stage (Lade et al. 1996; Feda 2002). Therefore, in the tests conducted on saturated and dry specimens, the time-dependent straining of the material is mainly associated with the microlevel rearrangement of the grain fabric resulting in a gradual stabilization of the particulate medium. After each increase in the axial stress, the axial strain occurred with instantaneous settlement followed by a time-dependent strain that developed at a decaying rate.

The viscoplastic model parameters associated with a Perzyna—Lemaître—Chaboche model were determined by carry-

ing out different simulations and comparing the numerical results with their experimental counterparts obtained from three load steps. In order to quantify the model parameters, the elastic part of the strain increment was determined in each loading step, from the instantaneous deformation of the sample. The strain hardening parameter m was established from the variation of the equivalent viscoplastic strain with time. The viscosity coefficient A and stress exponent n, which are linked by a simple relationship, can be obtained by assuming one parameter to be constant. In this study, the stress exponent was considered constant and a reference stress was assumed; this enabled the derivation of the parameters by introducing a single unit for the viscosity coefficient.

The compression behavior of the material was computationally modeled for the last two load steps using the viscoplastic parameters selected from the estimated range. Comparing these results with the experimental data, it was shown that the parameters derived from the proposed procedure can reasonably predict the viscous oedometric compression of the ballotini samples at higher stress levels.

Acknowledgments

The writers are indebted to the reviewers for their constructive comments that led to considerable improvements in the interpretation and presentation of the experimental data. The work described in this paper was supported by a NSERC Discovery Grant awarded to A. P. S. Selvadurai.

Notation

The following symbols are used in this paper:

A = viscosity coefficient;
C^e_{ijmn} = elastic compliance tensor;
E = elastic modulus;
e_i = void ratio of the triaxial samples prior to application of deviator stress;
F = static yield function;
f = plastic function;
G = viscoplastic potential;
J_{2D} = second invariant of the deviatoric stress tensor;
m = strain hardening parameter;
n = stress exponent;
q = equivalent deviatoric stress;
q^* = reference stress;
S = axis of symmetry;
S_{ij} = deviatoric stress tensor;
ε^c_{rr} = viscoplastic strain in radial direction;
ε^c_{zz} = viscoplastic strain in axial direction;
$\dot{\varepsilon}_{ij}$ = tensor of the total strain rate;
$\dot{\varepsilon}^c_{ij}$ = tensor of the viscoplastic strain rate;
$\dot{\varepsilon}^e_{ij}$ = tensor of the elastic strain rate;
$\tilde{\varepsilon}^c$ = equivalent viscoplastic strain;
κ = hardening parameter;
ν = Poisson's ratio;
σ_C = confining stress;
σ_{ij} = tensor of total stress;
σ'_{ij} = tensor of effective stress;
σ_1 = maximum principal stress; and
Φ = flow function.

References

AnhDan, L., Tatsuoka, F., and Koseki, J. (2006). "Viscous effects on the stress-strain behavior of gravelly soil in drained triaxial compression." *Geotech. Test. J.*, 29(4), 330–340.

Cheng, Y. P., White, D. J., Bowman, E. T., Bolton, M. D., and Soga, K. (2001). "The observation of soil microstructure under load." *Proc., 4th Int. Conf. on Micromechanics of Granular Media (Powders & Grains*), Sendai, Japan, Balkema, Rotterdam, 69–72.

Cristescu, N., and Suliciu, I. (1982). *Viscoplasticity—Mechanics of plastic solids*, Springer, New York.

Davis, R. O., and Selvadurai, A. P. S. (1996). *Plasticity and geomechanics*, Cambridge University Press, Cambridge, Mass.

Desai, C. S., and Siriwardane, E. J. (1984). *Constitutive laws for engineering materials: With emphasis on geologic materials*, Prentice-Hall, Englewood Cliffs, N.J.

Desai, C. S., and Zhang, D. (1987). "Viscoplastic model for geologic materials with generalized flow rule." *Int. J. Numer. Analyt. Meth. Geomech.*, 11(6), 603–620.

Di Benedetto, H., Tatsuoka, F., and Ishihara, M. (2002). "Time-dependent shear deformation characteristics of sand and their constitutive modeling." *Soils Found.*, 42(2), 1–22.

Di Prisco, C., and Imposimato, S. (1996). "Time dependent mechanical behaviour of loose sands." *Mech. Cohesive-Frict. Mater.*, 1(1), 45–73.

Feda, J. (2002). "Notes on the effect of grain crushing on the granular soil behaviour." *Eng. Geol. (Amsterdam)*, 63(1–2), 93–98.

Gajo, A., Piffer, L., and De Polo, F. (2000). "Analysis of certain factors affecting the unstable behaviour of loose sand." *Mech. Cohesive-Frict. Mater.*, 5(3), 215–237.

Hannink, G. (1994). "Settlement of high-rise buildings in Rotterdam." *Proc., 13th Int. Conf. on Soil Mechanics and Foundation Engineering*, Balkema, New Delhi, India, 441–444.

Komornik, A., Wiseman, G., and Zeitlen, J. G. (1972). "Building settlement on end-bearing driven piles." *Proc., Conf. on Performance of Earth and Earth-Supported Structures*, Lafayette, Ind., ASCE, New York, 1135–1153.

Kuwano, R., and Jardine, R. J. (2002). "On measuring creep behaviour in granular materials through triaxial testing." *Can. Geotech. J.*, 39(5), 1061–1074.

Lade, P. V. (1994). "Creep effects on static and cyclic instability of granular soils." *J. Geotech. Engrg.*, 120(2), 404–419.

Lade, P. V., and Liu, C.-T. (1998). "Experimental study of drained creep behavior of sand." *J. Eng. Mech.*, 124(8), 912–920.

Lade, P. V., Yamamuro, J. A., and Bopp, P. A. (1996). "Significance of particle crushing in granular materials." *J. Geotech. Engrg.*, 122(4), 309–316.

Lemaître, J., and Chaboche, J. L. (1996). *Mécanique des matériaux solides*, Dunod, Paris.

Leung, C. F., Lee, F. H., and Yet, N. S. (1996). "The role of particle breakage in pile creep in sand." *Can. Geotech. J.*, 33(6), 888–898.

Mitchell, J. K., and Solymar, Z. V. (1984). "Time-dependent strength gain in freshly deposited or densified sand." *J. Geotech. Engrg.*, 110(11), 1559–1576.

Murayama, S. (1983). "Formulation of stress-strain-time behavior of soils under deviatoric stress condition." *Soils Found.*, 23(2), 43–57.

Murayama, S., Michihiro, K., and Sakagami, T. (1984). "Creep characteristics of sands." *Soils Found.*, 24(2), 1–15.

Nawir, H., Tatsuoka, F., and Kuwano, R. (2003). "Experimental evaluation of the viscous properties of sand in shear." *Soils Found.*, 43(6), 13–31.

Nonveiller, E. (1963). "Settlement of a grain silo on fine sand." *Proc., 3rd European Conf. on Soil Mechanics and Foundation Engineering*, Wiesbaden, Germany, Deutsche Gesellschaft fur Erdund Grundbau, 285–294.

Oda, M. (1972). "The mechanism of fabric changes during compressional deformation of sand." *Soils Found.*, 12(2), 1–18.

Palmeira, E. M., and Gardoni, M. G. (2002). "Drainage and filtration

properties of non-woven geotextiles under confinement using different experimental techniques." *Geotext. Geomembr.*, 20(2), 97–115.
Perzyna, P. (1966). "Fundamental problems in visco-plasticity." *Advances in applied mechanics*, Academic, New York, 243–377.
Schmertmann, J. H. (1991). "Mechanical aging of soils." *J. Geotech. Engrg.*, 117(9), 1288–1330.
Selvadurai, A. P. S., and Sepehr, K. (1999). "Two-dimensional discrete element simulations of ice-structure interaction." *Int. J. Solids Struct.*, 36(31–32), 4919–4940.
Sweeney, M., and Lambson, M. D. (1991). "Long term settlements of storage tanks on sand." *Proc., 10th European Conf. on Soil Mechanics and Foundation Engineering*, Florence, Italy, 587–591.
Yamamuro, J. A., and Lade, P. V. (1993). "Effects of strain rate on instability of granular soils." *Geotech. Test. J.*, 16(3), 304–313.